First Results of Gas-Puff Imaging of Edge Turbulence in the W7-X Stellarator

S.B. Ballinger[1], S.G. Baek[1], C. Killer[2], A. von Stechow[2], J.L. Terry[1], O. Grulke[2,3], and the W7-X Team

[1]*Massachusetts Institute of Technology, Cambridge, MA, USA;* [2]*Max Planck Institut für Plasmaphysik, Greifswald, Germany;* [3]*Technical University of Denmark, Lyngby, Denmark*

Background The dynamics of filaments in the scrape-off layer (SOL) of the W7-X stellarator are important to understand turbulence and transport in this region. Several diagnostics on W7-X have characterized filaments and drift effects in the SOL, finding mainly poloidal propagation consistent with the $\mathbf{E}_r \times \mathbf{B}$ drift, with velocities of several km/s [1, 2, 3, 4, 5, 6]. These are complemented by a new gas-puff imaging (GPI) diagnostic, which offers 2D, high time-resolution, toroidally localized recordings of turbulent structures. Two supersonic nozzles puff neutral hydrogen or helium gas locally at the outboard side of the plasma, and line radiation resulting from the interaction of the boundary plasma with the puffed gas is recorded by an 8×16 pixel avalanche photodiode camera at 2 MHz [7]. We present the first results from the W7-X run campaign OP2.1.

Analysis methods Feature motion is more clearly revealed in GPI recordings by subtracting the running average from each pixel. Features are typically between 1–3 cm in size (figure 1).

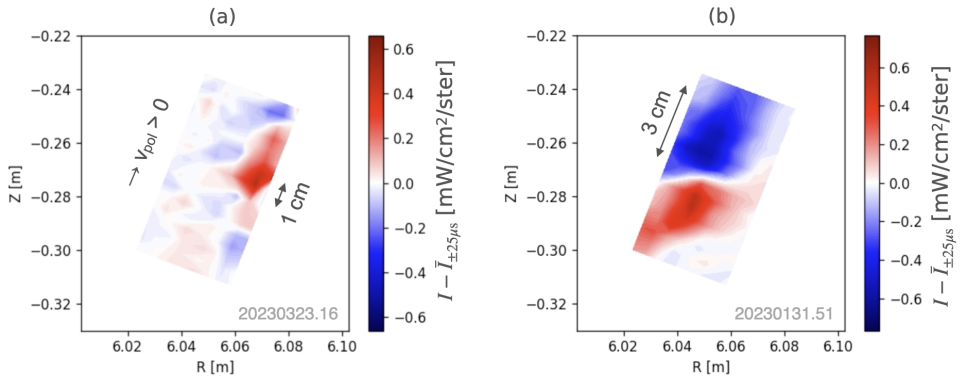

Figure 1: (a) small structures (likely filaments) and (b) large structure (likely a mode) in background-subtracted GPI videos.

Poloidal motion is much more apparent by eye than radial motion in the majority of GPI recordings. Spatio-temporal Fourier analysis is used to estimate the poloidal propagation velocities of features. A frequency-wavenumber spectrum is calculated for each column of pixels, which are oriented so that they are approximately parallel to the last closed flux surface, and coherent phase velocities appear as lines with $\omega = v_{\mathrm{ph}} k$. This spectrum is integrated over ranges

of v_{ph} to create a probability density function (PDF) of phase velocity, and the dominant phase velocity is taken to be that for which the PDF is maximum.

Impact of magnetic field configuration W7-X has a large number of available magnetic configurations, of which the most commonly used are the standard, high mirror, and low and high iota configurations. These were compared by computing the poloidal phase velocity of features moving along each column of the detector over a 50 millisecond period around the time of peak brightness, for all discharges with usable GPI data in forward magnetic field and with any control coil currents. In all configurations, the poloidal speeds evaluated in this way are typically between 1–5 km/s (figure 2(a)). The typical emission fluctuation amplitude is less than 20% of the mean (figure 2(b)). This analysis cannot be used to make blanket statements about the relative amount of edge turbulence in each configuration, as GPI views a different part of the SOL in each one: an island O-point in the standard and high-mirror configurations, an X-point in low iota (figure 3), and the far SOL in high iota. As shown later, the toroidal current also influences the extent of the SOL viewed by GPI, and figure 2 includes measurements at low and high toroidal currents.

Figure 2: Histograms of (a) the poloidal phase velocity, with the analysis from each column of the detector counted separately and (b) the root mean square divided by the mean, with the analysis of each detector pixel counted separately.

Typical flow patterns As noted earlier, poloidal motion typically dominates radial motion in the fluctuation dynamics. In the standard configuration, with GPI viewing across the O-point of an island, up to 3 shear layers are typically observed in the radial profile of the poloidal velocities (figure 3(a)). When the toroidal field direction is reversed, all these velocities also reverse, offering strong evidence that they are due to the $\mathbf{E}_r \times \mathbf{B}$ drift. The electric potential profile implied by figure 3(a), assuming all velocities are due to $\mathbf{E}_r \times \mathbf{B}$ motion, is qualitatively supported by reciprocating probe measurements of the floating potential under the same conditions.

A series of experiments was performed in which the O-point was moved up and down